HHS Public Access

Author manuscript

Cancer Res. Author manuscript; available in PMC 2017 April 01.

Published in final edited form as:

Cancer Res. 2016 April 1; 76(7): 1869–1881. doi:10.1158/0008-5472.CAN-15-1911.

Deletion of interstitial genes between *TMPRSS2* and *ERG* promotes prostate cancer progression

Douglas E. Linn[1], **Kathryn L. Penney**[2,3], **Roderick T. Bronson**[4], **Lorelei A. Mucci**[2,3], and **Zhe Li**[1,*]

[1]Division of Genetics, Brigham and Women's Hospital and Department of Medicine, Harvard Medical School, Boston, Massachusetts 02115, USA

[2]Channing Division of Network Medicine, Brigham and Women's Hospital and Department of Medicine, Harvard Medical School, Boston, Massachusetts 02115, USA

[3]Department of Epidemiology, Harvard School of Public Health, Boston, Massachusetts 02115, USA

[4]Rodent Histopathology, Harvard Medical School, Boston, Massachusetts 02115, USA

Abstract

TMPRSS2-ERG gene fusions that occur frequently in human prostate cancers can be generated either through insertional chromosomal rearrangement or by intrachromosomal deletion. Genetically, a key difference between these two mechanisms is that the latter results in deletion of a ~3Mb interstitial region containing genes with unexplored roles in prostate cancer. In this study, we characterized two mouse models recapitulating *TMPRSS22-ERG* insertion or deletion events in the background of prostate-specific PTEN deficiency. We found that only the mice which lacked interstitial region developed prostate adenocarcinomas marked by poor differentiation and epithelial-to-mesenchymal transition. Mechanistic investigations identified several interstitial genes, including *Ets2* and *Bace2*, whose reduced expression correlated in the gene homologs in human prostate cancer with biochemical relapse and lethal disease. Accordingly, PTEN-deficient mice with prostate-specific knockout of *Ets2* exhibited marked progression of prostate adenocarcinomas that was partly attributed to activation of MAPK signaling. Collectively, our findings established that *Ets2* is a tumor suppressor gene in prostate cancer and its loss along with other genes within the *TMPRSS2-ERG* interstitial region contributes to disease progression.

Keywords

TMPRSS2-ERG gene fusion; interstitial deletion; tumor suppressor; mouse model; ETS2

[*]Corresponding author: Zhe Li, Division of Genetics, Brigham and Women's Hospital, 77 Avenue Louis Pasteur, Boston, MA 02115, USA. Phone: 617-525-4740; FAX: 617-525-4705; ; Email: zli4@rics.bwh.harvard.edu.

Conflict of interest: The authors declare no conflict of interest.

Introduction

Over half of Prostate-Specific Antigen (PSA)-screened prostate cancer (PCa) patients possess gene fusions involving members of the ETS transcription factor family (1, 2). In the United States, this translates to more than 120,000 men diagnosed with *ETS* fusion-positive PCa each year. The most common subtype of *ETS* fusion juxtaposes the androgen-regulated promoter of serine protease gene *TMPRSS2* with the coding region of an *ETS* gene, *ERG*, leading to *ERG* overexpression. Both *TMPRSS2* and *ERG* genes are located on human chromosome 21q22 and are separated by a 3Mb interstitial region. The *TMPRSS2-ERG* gene fusion is predominantly generated either through intrachromosomal deletion of this interstitial region (referred to as "deletion") or via chromosomal rearrangement through insertion of the interstitial region (referred to as "insertion") (3–6). As a whole, *ERG* rearrangements are believed to be a PCa-specific event (7, 8), yet their prognostic value to date remains controversial (9). Numerous studies found no association between *TMPRSS2-ERG* fusions and tumor grade, stage, Gleason score, PSA recurrence or mortality (9–12). A recent review and meta-analysis both have exhaustively summarized literature to date demonstrating the overall lack of consistent prognostic value for *TMPRSS-ERG* fusion in PCa (9, 12). Differences in patient cohorts, diagnosis method, and fusion detection method may account for these conflicting results. Nonetheless, it is important to note that since *TMPRSS2-ERG* fusions are thought to represent an early event in prostate tumorigenesis (2, 8), other oncogenic events that drive PCa progression to later stages may also contribute to differential clinical outcomes for patients with fusion-positive PCa. In addition, another important consideration is that *TMPRSS2-ERG* rearrangements are genetically distinct and may have different biological consequences. Various subclasses of *TMPRSS2-ERG* fusions have largely been grouped together in the literature, thus potentially masking their true prognostic value. For instance, it has been suggested that PCas with *TMPRSS2-ERG* fusions generated through deletion represent more aggressive cases than those with fusions formed via insertion (5). Furthermore, it was reported that patients with duplicated copies of deletion-generated fusions exhibited extremely poor survival (13). Lastly, in a rapid autopsy cohort, *TMPRSS2-ERG* fusions in fusion-positive metastases from patients with hormone-refractory PCa were uniformly generated through deletion (14). Collectively, it remains unclear whether interstitial deletion, which deletes one copy of the intervening genes between *TMPRSS2* and *ERG*, represents a separate genetic event that contributes to prostate tumorigenesis, and whether deletion alone or in conjunction with *TMPRSS2-ERG* fusion expression correlates with a more aggressive subtype of fusion-positive PCa. A better understanding of this may reveal novel tumor suppressor(s) in the interstitial region and enhance our understanding of the underlying biology of aggressive PCa.

The *TMPRSS2-ERG* interstitial region contains ~16 known protein-encoding genes (Supplementary Fig. S1), several of which have reported tumor-suppressive roles. A gene encoding another ETS factor, *ETS2*, is located in this region and its ectopic expression decreased proliferation and invasion of PCa cell lines (15, 16). HMGN1, which binds to and maintains an open chromatin configuration, plays a critical role in DNA repair; its loss led to increased N-Cadherin expression (17), a gene associated with high-grade PCa (18). In addition, *MX1* encodes an interferon-inducible GTPase MxA and its ectopic expression

drastically reduced the motility and invasiveness of an aggressive subline of PC3 PCa cells (19). Together, these studies suggest that deletion of one or more genes within this region may lead to haploinsufficiency or loss of expression, which may promote PCa progression.

To study the role of *TMPRSS2-ERG* fusions in PCa, we recently generated two knockin mouse models that recapitulate either *TMPRSS2-ERG* insertion or deletion events (20). Notably, prostate-specific activation of both conditional knockin alleles leads to expression of the same fusion transcript as the predominant *TMPRSS2-ERGa* subtype originally described by Tomlins et al (1), and the only genetic difference is that one model has deletion of the interstitial region, whereas the other has no deletion. Importantly, these interstitial regions are syntenic between human and mouse with almost all known protein-encoding genes being conserved (Supplementary Fig. S1). Thus, these models offer a unique opportunity to study whether the interstitial deletion also represents a genetic event that contributes to prostate tumorigenesis. In this study, we compared the prostate phenotypes of these two models under the background of *Probasin-Cre* (*Pb-Cre*)-mediated biallelic *Pten* inactivation, and provided genetic evidence that reduced expression of the interstitial genes, in particular, *ETS2*, promotes PCa progression. We also explored associations of the interstitial genes in PCa cohorts to test their clinical relevance.

Materials and Methods

Mouse strains, procedures, and tissue preparation

T-ERG and *T-3Mb-Erg* knockin mice were generated previously (20). *Pb-Cre* (*Pb-Cre4*) transgenic mice were obtained from the Mouse Models of Human Cancers Consortium (MMHCC) repository. *Rosa26-STOP-YFP* (*R26YFP*) conditional Cre-reporter mice, *Pten* and *Ets2* conditional knockout mice ($Pten^{L/L}$, $Ets2^{L/L}$) were obtained from The Jackson Laboratory (JAX). All mice were maintained on a mixed genetic background and housed in pathogen-free barrier environment. All mouse studies were approved by the Institutional Animal Care and Use Committee (IACUC). Prostate tissues used for immunohistochemistry (IHC) were fixed for 16 hours in 10% formalin (Fisher), dehydrated, and embedded in paraffin. Tissues used for immunofluorescent (IF) staining were fixed in 10% formalin for 1 hour, washed in PBS, then saturated in 30% sucrose overnight at 4°C. Tissues were then embedded in OCT compound (Sakura) and stored at −80°C prior to cryosectioning.

Histology, immunohistochemistry and immunofluorescent staining

Paraffin-embedded tissues were stained with H&E and reviewed by a trained rodent histopathologist. Pathology was defined as previously described (21, 22). IHC was carried out by rehydrating sections, performing antigen unmasking with Tris-EDTA buffer. Sections were blocked with 2.5% goat serum for 1 hour at room temperature and incubated with primary antibodies overnight at 4°C. Antibodies for IHC were used to detect ERG (Epitomics 2805), AR (Santa Cruz sc816), SMA (Sigma A2547), p63 (Chemicon MAB4135), E-Cadherin (Cell Signaling 3195), Vimentin (abcam 92547), ETS2 (Santa Cruz sc351), HMGN1 (abcam 5212), or BACE2 (abcam 5670). Staining was visualized using DAB substrate (Vector) and counter-stained with hematoxylin. Slides were dehydrated and sealed using Permount mounting media (Fisher). For IF staining, cryosections of prostate

tissues were sectioned at 8μm, blocked in 2.5% goat serum, and incubated with primary antibodies overnight at 4°C. Antibodies for IF were used to detect YFP (abcam 13970), Vimentin (abcam 92547), K5 (Covance PRB-160P) or K8 (Covance MMS-162P). Alexa Fluor-conjugated secondary antibodies (Life Technologies) were incubated for 1 hour at room temperature. Nuclei were counterstained with DAPI and slides were sealed with Vectashield mounting media (Vector).

Laser capture microdissection and gene expression profiling

Paraffin-embedded prostates were stained with hematoxylin and excised using the ArcturusXT Laser Capture Microdissection system to collect genomic DNA or total RNA. DNA was isolated using the Arcturus PicoPure kit (Life Technnologies) and RNA was isolated using the RNeasy FFPE kit (Qiagen). Nucleic acid quality was validated on a BioAnalyzer (Agilent) and samples were processed using the Ovation RNA Amplification System (NuGEN) prior to gene expression profiling with the Affymetrix Mouse Gene 2.0 ST chip.

Prostate regeneration assays

In vivo prostate regeneration assays were performed as previously described (23). Briefly, prostate epithelial cells were dissociated and MACS-sorted (Miltenyi Biotec) to removed Lineage positive cells (CD31, CD45, Ter119). Cre-naiive cells used for PCa initiation studies were infected with *CMV-Cre* adenovirus (50 MOI, from University of Iowa Gene Transfer Core) for 1 hour at 37°C. Approximately 2.5 x 10^5 sorted cells were mixed with 2.5 x 10^5 Urogenital sinus mesenchyme (UGSM) cells and subcutaneously injected with Matrigel into flanks of *Rag2*-deficient mice. Outgrowths were collected 8 weeks post injection.

Cell culture, shRNA knockdown and Western blot

VCaP cell line was purchased from American Type Culture Collection (<5 years ago) and was authenticated again internally by Short Tandem Repeat (STR) profiling test; it was free from mycoplasma contamination and was cultured in DMEM medium with 10%FBS. VCaP cells were stably transduced by pGIPZ lentiviruses with shRNAs for *ETS2* [shETS2_1: V3LHS_646035; shETS2_2: V3LHS_642164, or with control shRNA (empty vector pGIPZ shRNA, #RHS4351), from Open Biosystems]. Western blot was performed as previously described (24) on lysates were collected 72 hours post-infection. Antibodies used include, from Cell Signaling: pMET (3077), total MET (3127), pERK1/2 (4370), total ERK1/2 (9102), GAPDH (2118), and from Santa Cruz: ETS2 (sc351).

Data analysis

Hierarchical clustering and heatmaps were generated using MultiExperiment Viewer. Statistical significance was calculated using Student's t-test. GSEA was performed as described (25). Analysis of human data was performed using cbio-portal.

For the PHS and HPFS analysis, we utilized data from a gene expression profiling study. Briefly, men were sampled from the HPFS and PHS Prostate Tumor Cohort using an extreme case design, which includes 119 men who died of their cancer or developed bony or

distant metastases ("lethal") and 282 men who lived at least 8 years after PCa diagnosis and were not diagnosed with metastases through 2012 ("indolent"). Briefly, RNA was extracted from tissue, then amplified using the WT-Ovation FFPE System V2 (NuGEN), a whole transcriptome amplification system that allows for complete gene expression analysis from archives of FFPE samples. After reverse transcription and fragmentation, the cDNA was hybridized to the Affymetrix GeneChip Human Gene 1.0 ST microarray. After normalization of the data, we mapped gene names to Affymetrix transcript cluster IDs using the NetAffx annotations as implemented in Bioconductor annotation package pd.hugene. 1.0.st.v1. We compared the expression of the interstitial genes across the lethal and indolent cases using linear regression.

Accession numbers

The microarray expression profiling data set generated in this manuscript has been deposited to the GEO database under the following accession number: GSE63070.

Results

Tmprss2-Erg fusion with interstitial deletion more strongly cooperates with *Pten*-loss

We previously reported generation and characterization of two knockin mouse models of *Tmprss2-Erg* fusions for PCa (20). In the insertion model, an N-terminus truncated human *ERG* cDNA was knocked-in to the mouse *Tmprss2* locus directly (*Tmprss2-STOP-ERG*, Cre-mediated excision of the floxed *STOP* cassette leads to activation of the *Tmprss2-ERG* fusion allele; these are collectively referred to as "*T-ERG*" knockin). The second model utilized sequential gene targeting to introduce *loxP* sites into the mouse *Tmprss2* and *Erg* loci, respectively, thus allowing deletion of the entire interstitial region upon Cre recombinase expression (i.e., referred to as "*T-3Mb-Erg*" before Cre-mediated excision of the interstitial region, and "*T-Δ-Erg*" after excision). In the presence of a single copy of *Pten*-null allele, both lines expedited formation of low-grade Prostatic Intraepithelial Neoplasia (LG-PIN) at similar rates and exhibited indistinguishable phenotypes that rarely developed into higher grade lesions, but never to frank adenocarcinoma (20). In the presence of biallelic *Pten* inactivation mediated by *Pb-Cre*, however, most *Pb-Cre;T-3Mb-Erg;Pten*$^{L/L}$ male mice developed large poorly differentiated prostate tumors (i.e., *T-Δ-Erg/Pten*-null tumors) in dorsolateral and ventral lobes by 12 months of age (20). To determine whether this advanced PCa phenotype is caused by *Tmprss2-Erg* fusion expression or interstitial deletion, or both, we similarly generated *Pb-Cre;T-ERG;Pten*$^{L/L}$ males and characterized their prostate phenotype at 12 months of age. Intriguingly, none of the *Pb-Cre;T-ERG;Pten*$^{L/L}$ males developed poorly differentiated prostate adenocarcinoma at this age (Fig. 1A–B) [compared to almost 100% penetrance for *Pb-Cre;T-3Mb-Erg;Pten*$^{L/L}$ males to develop poorly and/or moderately differentiated adenocarcinomas (Fig. 1B)]. The prostate lesions developed in these males were quite similar to those high-grade PIN (HG-PIN) lesions often observed in *Pb-Cre;Pten*$^{L/L}$ control males at this age (Fig. 1A). Furthermore, control *Pb-Cre;Pten*$^{L/L}$ males and *Pb-Cre;T-ERG;Pten*$^{L/L}$ males only displayed signs of local invasion, which was confirmed through IHC staining of smooth muscle actin (SMA) (Fig. 1A). In stark contrast, *Pb-Cre;T-3Mb-Erg;Pten*$^{L/L}$ males developed invasive prostate tumors that lacked expression of SMA and basal marker p63 (Fig. 1A). Such *T-Δ-Erg/Pten*-null

tumors were positive for the prostate luminal epithelial marker Keratin 8 (K8), but were negative for the basal epithelial marker Keratin 5 (K5) (Fig. 1C). These *Pb-Cre;T-3Mb-Erg;Pten*$^{L/L}$ males also developed typical HG-PIN lesions composed of K8^{+} luminal cells surrounded by K5^{+} basal cells that are often observed in the control *Pb-Cre;Pten*$^{L/L}$ males (Fig. 1C), as well as localized invasive cancers with microducts mainly composed of K8^{+} prostate luminal cells [with almost no K5^{+} basal cells (Fig. 1C), and almost no SMA and p63 expression (Supplementary Fig. S2A)]. Poorly differentiated adenocarcinomas were never observed in control *Pb-Cre;Pten*$^{L/L}$ or *Pb-Cre;T-ERG;Pten*$^{L/L}$ males, whereas presence of invasive microducts consistent with moderately differentiated adenocarcinoma were only infrequently detected in these controls (Fig. 1B).

Adenocarcinomas and HG-PINs developed in *Pb-Cre;T-3Mb-Erg;Pten*$^{L/L}$ mice exhibit Cre-mediated interstitial deletion

By IHC staining, we confirmed that ERG protein was robustly expressed in HG-PIN lesions developed in both *Pb-Cre;T-ERG;Pten*$^{L/L}$ and *Pb-Cre;T-3Mb-Erg;Pten*$^{L/L}$ males (Supplementary Fig. S2B). We previously reported that in *Pb-Cre;T-3Mb-Erg;Pten*$^{L/L}$ male mice, moderately differentiated invasive cancers with microducts developed in their prostates often exhibited a mosaic pattern of ERG protein expression, whereas poorly differentiated invasive adenocarcinomas were largely negative for ERG (20). To rule out a possibility in which lack of ERG expression is due to reduced efficiency in generating *Tmprss2-Erg* fusion from Cre-mediated deletion of the large 3Mb interstitial region in the conditional *T-3Mb-Erg* allele, we performed laser capture microdissection to isolate epithelial cells from well-defined regions of either HG-PIN (mainly ERG positive) or poorly differentiated adenocarcinoma (tumor, mainly ERG negative) (Supplementary Fig. S3). We then extracted genomic DNA from these isolated tissues as well as from the whole prostates (i.e., containing both ERG positive and negative lesions) and by genomic DNA PCR analysis (Supplementary Fig. S4A), we verified that in both types of tissues, the *Tmprss2-Erg* gene fusion was generated effectively via Cre-mediated interstitial deletion (Supplementary Fig. S4B). This data suggests that advanced PCa lesions observed in the *Pb-Cre;T-3Mb-Erg;Pten*$^{L/L}$ model are most likely due to the interstitial deletion between the *Tmprss2* and *Erg* loci.

T-Δ-Erg/Pten-null tumors exhibit an EMT phenotype

To investigate the biological mechanism underlying the more aggressive *T-ΔErg/Pten*-null tumors, we performed gene expression profiling using laser capture microdissected prostate epithelial cells. Only cells with round epithelial-like morphology were excised leaving behind spindle-shaped mesenchymal cells. As an internal control for stage-specific differences between cancer lesions developed in control *Pb-Cre;Pten*$^{L/L}$ males (i.e., mainly HG-PIN) and *Pb-Cre;T-3Mb-Erg;Pten*$^{L/L}$ males [i.e., poorly differentiated adenocarcinoma (tumor) and HG-PIN], we also excised HG-PIN lesions (in addition to tumors) from *Pb-Cre;T-3Mb-Erg;Pten*$^{L/L}$ mice for analysis (Supplementary Fig. S3). Among genes differentially regulated between these three groups, gene set enrichment analysis (GSEA) (25) revealed that multiple previously defined epithelial-to-mesenchymal transition (EMT) gene sets were enriched in *T-Δ-Erg/Pten*-null tumors compared to control *Pten*-null HG-PIN lesions (Fig. 2A and Supplementary Fig. S5A). Enrichment of EMT gene sets could also be

found when comparing *T-Δ-Erg/Pten*-null HG-PIN lesions to *Pten*-null HG-PIN lesions (Supplementary Fig. S5B), or when comparing *T-Δ-Erg/Pten*-null tumors to HG-PIN lesions developed in the same mice (Supplementary Fig. S5C). These analyses suggested that the EMT signature in the *T-Δ-Erg/Pten*-null tumors was not simply due to a tumor stage difference (i.e., poorly differentiated adenocarcinoma versus HG-PIN), but was acquired progressively during PCa progression when under the interstitial deletion background. We validated the EMT signature using IHC for E-Cadherin and Vimentin, which display epithelial and stromal compartment-restricted expression, respectively (Fig. 2B). E-Cadherin was highly expressed in the epithelial compartment in HG-PIN lesions in *Pb-Cre;Pten*$^{L/L}$, *Pb-Cre;T-ERG;Pten*$^{L/L}$ and *Pb-Cre;T-3Mb-Erg;Pten*$^{L/L}$ mice, but was downregulated in *T-ΔErg/Pten*-null tumors. Inversely, Vimentin displayed stromal-specific expression in all HG-PIN lesions yet was abundant within epithelial cells of the *T-Δ-Erg/Pten*-null tumors. In these *Pb-Cre*-based mice, a conditional Cre-reporter *Rosa26-STOP-YFP* (*R26Y*, Cre-mediated excision of a floxed *STOP* cassette in this allele leads to activation of the YFP reporter) was included to track *Pb-Cre*-expressing cells and their daughter cells (i.e., YFP$^+$ prostate epithelial cells). The presence of EMT features was also verified in IF analyses where the epithelial marker K8 and the lineage marker YFP (for genetic marking) overlapped with Vimentin only in tumor cells but not in HG-PIN lesions (Supplementary Fig. S5D). This data suggested that although the EMT program was already upregulated in *T-Δ-Erg/Pten*-null HG-PIN lesions at the transcript level, changes in the expression of key EMT markers at the protein level appeared at later tumor stages. Lastly, to rule out a possibility in which the poorly differentiated tumors with mesenchymal features developed in *Pb-Cre;T-3Mb-Erg;Pten*$^{L/L}$ mice were due to a desmoplastic response in the stroma (as a response to invasive PCa developing nearby), similar to what was reported for the *Pb-Cre;T-ETV1;Pten*$^{L/L}$ mouse model (20), we stained these tumors for YFP expression and found that they were indeed YFP$^+$ (Supplementary Fig. S5E), thus confirming that these large poorly differentiated *T-ΔErg/Pten*-null tumors were derived from *Pb-Cre*-mediated recombination and therefore of epithelial origin.

T-Δ-Erg/Pten-null tumors retain partial AR signaling

Similar to the *Pb-Cre;T-3Mb-Erg;Pten*$^{L/L}$ model, mice with *Pb-Cre*-induced *Pten*-loss and RAS/MAPK activation also develop poorly differentiated prostate tumors with an EMT phenotype (i.e., *Ras/Pten* tumors) (26). These *Ras/Pten* tumors exhibited highly heterogeneous androgen receptor (AR) expression and overall reduced expression of AR target genes (26). To determine the status of AR signaling in *T-Δ-Erg/Pten*-null prostate tumors, we stained them for AR protein expression and found that *T-ΔErg/Pten*-null tumors are largely AR positive (Fig. 3A). By analyzing microarray expression data, we found that expression of *Nkx3-1*, a well-known AR target and tumor suppressor gene, was not significantly changed in *T-Δ-Erg/Pten*-null tumors or HG-PIN lesions compared to *Pten*-null HG-PIN lesions; *Fkbp5*, a recently described AR target gene that mediates reciprocal inhibition between PTEN/PI3K and AR pathways (27, 28), was slightly upregulated in *T-Δ-Erg/Pten*-null tumors compared to *Pten*-null HG-PINs (Fig. 3B). In contrast, these two AR target genes both exhibited a trend of downregulation in *Ras/Pten* tumors compared to *Pten*-null lesions [Supplementary Fig. S6A and (26)]. However, several other AR target genes related to normal prostate function, including *Mme*, *Msmb* and *Tmprss2*, all exhibited a

trend of downregulation in both *T-Δ-Erg/Pten*-null and *Ras/Pten* tumors in relation to *Pten*-null lesions [Fig. 3C, Supplementary Fig. S6A and (26)]. Of note, downregulation of *Tmprss2* in *T-Δ-Erg/Pten*-null prostate tumors in relation to both *T-Δ-Erg/Pten*-null and *Pten*-null HG-PIN lesions may explain downregulation of *Erg* expression (which is under the control of the endogenous *Tmprss2* promoter) in *T-Δ-Erg/Pten*-null tumors, but not in *T-Δ-Erg/Pten*-null HG-PIN lesions (20). Lastly, by GSEA using an androgen-driven signature we developed recently from human PCa cell lines (20), we found that this gene set exhibited a higher level of downregulation in *Ras/Pten* tumors than in *T-Δ-Erg/Pten*-null tumors, when compared to their corresponding *Pten*-null controls (Supplementary Fig. S6B–C). Collectively, these data suggest that compared to the *Ras/Pten* EMT tumors, *T-ΔErg/Pten*-null tumors retain expression of both AR and some of the AR target genes, but also exhibit downregulation of other AR targets. This is consistent with the concept of AR cistrome reprogramming in which AR binding sites change during PCa progression, when its collaborating factors are altered (e.g., due to different oncogenic events), leading to changes in the expression of select AR target genes (29).

Multiple interstitial genes are candidate prostate tumor suppressors

We next examined whether some interstitial genes could function as tumor suppressors during prostate carcinogenesis to explain the aggressive nature of *T-ΔErg/Pten*-null tumors. To do this, we first generated an “Interstitial genes” gene set composed of protein-coding genes between *TMPRSS2* and *ERG* and then performed GSEA using this gene set. We found that it was significantly downregulated in *T-ΔErg/Pten*-null tumors when compared to either *Pten*-null HG-PINs (Fig. 4A) or *T-ΔErg/Pten*-null HG-PINs (Fig. 4B). Among the downregulated interstitial genes, *Ets2* is abundantly expressed in prostate tissues [whereas several other ETS factor genes, such as *Ets1*, *Erg*, and *Etv1*, are not (Supplementary Fig. S7)] and its overexpression was shown previously to decrease proliferation and invasion of PCa cell lines (15, 16); however, other interstitial genes, such as *Bace2* and *Brwd1*, have so far not been implicated in PCa development. We analyzed expression of interstitial genes *Ets2*, *Hmgn1*, and *Bace2* in *T-Δ-Erg/Pten*-null HG-PIN and adenocarcinoma at the protein level (Fig. 4C). *Bace2* was included as it is the most significantly downregulated gene in the above GSEA analysis (Fig. 4A–B). Although *Hmgn1* failed to show up in the GSEA analysis (due to absence of *Hmgn1* probe conversion), we also included it in our validation, as it has been implicated in PCa as a potential tumor suppressor (17, 18). Expression at the protein level from these genes was abundantly detected in nuclei and cytoplasm of epithelial cells in HG-PIN lesions. In advanced tumors, expression levels were dramatically decreased, although weak cytoplasmic staining could still be observed (Fig. 4C). Interestingly, in our GSEA analysis, although the “Interstitial genes” gene set was not significantly enriched in HG-PIN lesions from *Pb-Cre;T-3Mb-Erg;Pten*$^{L/L}$ mice to those from *Pb-Cre;Pten*$^{L/L}$ control mice, the above-described interstitial genes such as *Ets2*, *Bace2* and *Brwd1* all exhibited a trend toward slight downregulation in *T-ΔErg/Pten*-null HG-PINs (Supplementary Fig. S8 and Table S1).

To determine whether reduced expression of interstitial genes is associated with PCa patient outcomes, we analyzed potential association of deletion of interstitial genes with biochemical relapse after radical prostatectomy in a previously published human PCa patient

cohort (30). We found that in this cohort, only 4 of 17 interstitial genes including *ETS2*, *BRWD1*, *HMGN1*, and *BACE2* were significant for PCa progression (when downregulated), regardless of patient fusion status (Fig. 4D). Patients possessing downregulation of the remaining set of interstitial genes did not exhibit differences in biochemical recurrence compared to those with normal expression levels. Similarly, *ERG* overexpression was not associated with time to failure (Fig. 4D). Lastly, we examined the potential clinical association of interstitial genes with lethal PCa in a larger study with 119 lethal PCa cases, defined as men with metastatic disease or cancer death, and 282 indolent cases with no evidence of metastatic disease [from the Physicians' Health Study (PHS) and the Health Professionals Follow-up Study (HPFS) (12, 31)]. We found that at least one-third of the interstitial genes, including *ETS2* and *BACE2*, are expressed at significantly lower levels in lethal PCa cases than indolent cases (Table 1). Collectively, these analyses suggest that multiple genes within the *TMPRSS2-ERG* interstitial region are associated with lethal PCa (when downregulated) and may function as tumor suppressors for PCa.

Reduced gene dosage of *Ets2* contributes to prostate cancer progression

Interstitial genes exhibiting significantly lower expression levels in advanced PCa (e.g., *ETS2*, *BACE2*) can either directly contribute to prostate tumorigenesis as a tumor suppressor or serve as a biomarker for lethal PCa, or both. To distinguish between these possibilities, we focused on *ETS2*, which is strongly downregulated in prostate tumors compared to benign tissues [(32) and in our PHS/HPFS study (*P-value*=$8.4x10^{-14}$)] and is also the most significantly downregulated interstitial gene in lethal PCas (Table 1). We crossed mice carrying a conditional knockout allele of *Ets2* (*Ets2*^{L}) (33) with *Pten*$^{L/L}$ mice to generate *Ets2*$^{L/+}$;*Pten*$^{L/L}$ male mice. We then performed the regeneration assay upon *ex vivo* exposure of their prostate cells to *CMV-Cre* adenovirus (*Ad-CMV-Cre*). *Ad-CMV-Cre*-infected *Pten*$^{L/L}$ control cells formed largely normal ducts with occasional areas of hyperplasia (Fig. 5A). In contrast, *Ad-CMV-Cre*-infected *Ets2*$^{L/+}$;*Pten*$^{L/L}$ prostate cells formed small proliferating lesions invading into the lumen, consistent with HG-PIN (Fig. 5A). Next, we generated *Pb-Cre;Ets2*$^{L/+}$;*Pten*$^{L/L}$, *Pb-Cre;Ets2*$^{L/L}$;*Pten*$^{L/L}$, and matched control *Pb-Cre;Pten*$^{L/L}$ male mice. At 6–9 months of age, we found that although the anterior lobes of all these mice developed HG-PIN lesions of comparable severity, the phenotypes from the dorsolateral and ventral lobes of the *Pb-Cre;Ets2*$^{L/+}$;*Pten*$^{L/L}$ and *Pb-Cre;Ets2*$^{L/L}$;*Pten*$^{L/L}$ males were notably stronger. Loss of one copy of *Ets2* resulted in development of larger HG-PIN lesions in both the dorsolateral and ventral lobes and the dorsolateral lobes also contained significantly more stromal proliferation and inflammatory infiltrate (Fig. 5B). Importantly, loss of both copies of *Ets2* led to emergence of poorly differentiated prostate adenocarcinoma in the ventral lobes (Fig. 5C). Collectively, these data suggest that *Ets2* is a tumor suppressor in PCa and its reduced dosage in prostate epithelial cells promotes PCa progression.

ETS2-loss leads to activation of the MAPK pathway

To determine how reduced *Ets2* dosage contributes to PCa progression, we further analyzed the microarray data from our animal models, focusing on comparing *T-Δ-Erg/Pten*-null HG-PINs to *Pten*-null HG-PINs (thus stage-matched). By GSEA, we found that in addition to the above-described EMT-related gene sets (Supplementary Fig. S5B), gene sets related to the

RAS/MAPK pathway, HGF/MET pathway, and WNT signaling, were also significantly enriched in *T-Δ-Erg/Pten*-null HG-PIN lesions (Fig. 6A and Supplementary Table S2). Interestingly, a recent study examining a tumor suppressor role of ETS2 in non-small cell lung cancer demonstrated association of ETS2-loss with activation of both HGF/MET and MAPK signaling, as well as induction of EMT-related genes (34). To determine whether ETS2-loss could induce similar pathway activation in PCa cells, we used shRNAs to knockdown *ETS2* expression in VCaP cells, which carry the *TMPRSS2-ERG* fusion without the interstitial deletion (1). We found that upon *ETS2* knockdown, the level of phosphorylated ERK1/2 (pERK1/2) was notably increased (Fig. 6B). Due to a low level of phosphorylated MET (pMET) in VCaP cells, we were unable to definitively determine whether reduced *ETS2* expression promotes activation of the HGF/MET pathway (data not shown). Collectively, our data from both animal models and human PCa cells suggest that ETS2-loss causes activation of at least the MAPK pathway, which cooperates with *Pten*-loss, leading to development of advanced PCa.

Discussion

Our unique mouse models have allowed examination and comparison of the biological consequences of *Tmprss2-Erg* fusions generated by insertion or deletion. ERG overexpression in the context of *Pten*-loss is sufficient for early initiation events as both models similarly expedited PIN frequency and severity in the context of a single copy of *Pten*-loss (20). However, the difference between these two models became obvious in aged mice when under the *Pten*-null background. Prostate lesions in *Pb-Cre;T-ERG;Pten*$^{L/L}$ males (i.e., no deletion) were histologically similar to those in control *Pb-Cre;Pten*$^{L/L}$ males and development of invasive PCa in either line was a relatively rare event. In stark contrast, *Pb-Cre;T-3Mb-Erg;Pten*$^{L/L}$ mice (i.e., with deletion) consistently developed poorly differentiated adenocarcinomas that exhibited EMT features and partial AR signaling. Together these data suggest that interstitial deletion may program prostate cells for development of more aggressive PCa than ERG overexpression alone. However, an important consideration is the prolonged delay for the phenotypic difference between *Pb-Cre;T-ERG;Pten*$^{L/L}$ and *Pb-Cre;T-3Mb-Erg;Pten*$^{L/L}$ males to emerge. This suggests that additional mutations or epigenetic events may be required for the full *T-Δ-Erg/Pten*-null phenotype to manifest. Another consideration is that ERG protein expression is largely lost in the poorly differentiated *T-Δ-Erg/Pten*-null tumors (20), whereas the majority of human PCas with *TMPRSS2-ERG* fusions retain ERG overexpression (35–38). However, a small subset of human fusion-positive castration-resistant cases (e.g., small cell/neuroendocrine PCa) were also found to be negative for ERG protein staining (39). Whether our *T-Δ-Erg/Pten*-null model recapitulates this subset of human PCa requires further investigation. Of note, a recent mouse model of prostate-specific ERG overexpression resulted in aggressive PCa (40), rather than HG-PIN lesions as observed in our *Pb-Cre;T-ERG;Pten*$^{L/L}$ model. This phenotypic difference may be due to a difference in how ectopic ERG expression is controlled: ERG overexpression in that mouse model is controlled by the constitutive *Rosa26* locus, whereas ERG overexpression in our *T-ERG* mouse model is driven by the endogenous *Tmprss2* control region, which is under regulation by both androgen and estrogen (20, 41, 42).

Our study provided definitive genetic evidence to support *ETS2* as a prostate tumor suppressor gene in the interstitial region. This is consistent with our epidemiological study demonstrating a significant association of *ETS2* downregulation with lethal PCa (Table 1), as well as findings from PCa genomes in which both focal deletion and point mutation of *ETS2* were identified in lethal castration-resistant PCa (16). Of note, ETS2 has also been shown as a tumor suppressor in other cancer types [e.g., colon cancer (43), lung cancer (34)]. Since both ERG and ETS2 belong to the ETS family of transcription factors that share the same or similar DNA-binding motif (44), it is possible that ectopic ERG expression may interfere with the normal function of ETS2 in prostate epithelial cells by competing with ETS2 for DNA binding. Thus, ETS factors (e.g., ETS2) normally expressed in prostate epithelial cells may serve as prostate tumor suppressors, whereas those ETS factors (e.g., ERG, ETV1, Supplementary Fig. S7) that are not expressed in prostate epithelial cells may serve as oncogenes (once ectopically expressed), by potentially interfering with functions of ETS factors normally expressed in prostate epithelial cells. This notion is consistent with the idea of an ETS transcriptional network in prostate tumorigenesis (45). Mechanistically, we showed that ETS2-loss might promote PCa progression in part via activation of the MAPK pathway. This is supported by the similar aggressive PCa phenotype (e.g., EMT) observed in both the *T-Δ-Erg/Pten*-null model and other mouse models with both *Pten*-loss and RAS/MAPK activation (26, 46).

Although our *T-Δ-Erg/Pten*-null model and the *Ras/Pten* model (26) both involve activation of the MAPK pathway, leading to development of prostate tumors with features of EMT, the EMT tumors developed in these models also exhibit difference at the molecular level (e.g., different AR activity and targets expression). Other deregulated pathways (e.g., due to ETS2-loss and/or loss of other tumor suppressor genes in the interstitial region) may contribute to this difference. In addition, although our *Pb-Cre;T-3Mb-Erg;Pten*$^{L/L}$ mice had only one copy of each interstitial gene deleted by Cre-mediated excision, the remaining alleles might also be additionally silenced through unidentified mechanisms. This might explain the lost expression of select interstitial genes (e.g., *Ets2*, *Hmgn1*, *Bace2*) in advanced PCa. Furthermore, recent study suggested that combinations of hemizygous deletions of multiple tumor suppressors might be required to produce maximal cancer phenotypes (47). This provides another potential mechanism for loss of multiple interstitial genes to contribute to prostate tumorigenesis jointly. Overall, although we have validated *ETS2* as a major tumor suppressor in this region, we cannot exclude that other interstitial genes (e.g., *BACE2*) may have tumor suppressor roles as well. Future characterization of clinical samples with careful dissection of the individual and combinatorial contribution of the loss of these candidate interstitial genes, coupled with mouse modeling, may reveal additional tumor suppressor(s) in this interstitial region. Lastly, our study also suggests that clinical prognostic studies may need to consider more carefully distinguishing *TMPRSS2-ERG* fusions based on deletion or insertion, as they may contribute to distinct clinical outcomes.

Supplementary Material

Refer to Web version on PubMed Central for supplementary material.

Acknowledgments

Financial support: This research was supported by NIH grant R01 CA136578 (to L.A.M.), and by a Career Development Award from Dana-Farber/Harvard Cancer Center Prostate Cancer SPORE (P50 CA090381) and Idea Development Awards from Department of Defense (W81XWH-11-1-0329, W81XWH-15-1-0546) (to Z.L.).

We would like to thank Xin Zhang for her assistance in maintaining and genotyping some of the mouse models and Drs. Esther Baena and Ying Xie for technical assistance with experimental assays.

References

1. Tomlins SA, Rhodes DR, Perner S, Dhanasekaran SM, Mehra R, Sun XW, et al. Recurrent fusion of TMPRSS2 and ETS transcription factor genes in prostate cancer. Science. 2005; 310:644–8. [PubMed: 16254181]
2. Kumar-Sinha C, Tomlins SA, Chinnaiyan AM. Recurrent gene fusions in prostate cancer. Nat Rev Cancer. 2008; 8:497–511. [PubMed: 18563191]
3. Teixeira MR. Chromosome mechanisms giving rise to the TMPRSS2-ERG fusion oncogene in prostate cancer and HGPIN lesions. Am J Surg Pathol. 2008; 32:642–4. author reply 4. [PubMed: 18317354]
4. Hermans KG, van Marion R, van Dekken H, Jenster G, van Weerden WM, Trapman J. TMPRSS2:ERG fusion by translocation or interstitial deletion is highly relevant in androgen-dependent prostate cancer, but is bypassed in late-stage androgen receptor-negative prostate cancer. Cancer Res. 2006; 66:10658–63. [PubMed: 17108102]
5. Perner S, Demichelis F, Beroukhim R, Schmidt FH, Mosquera JM, Setlur S, et al. TMPRSS2:ERG Fusion-Associated Deletions Provide Insight into the Heterogeneity of Prostate Cancer. Cancer Res. 2006; 66:8337–41. [PubMed: 16951139]
6. Yoshimoto M, Joshua AM, Chilton-Macneill S, Bayani J, Selvarajah S, Evans AJ, et al. Three-color FISH analysis of TMPRSS2/ERG fusions in prostate cancer indicates that genomic microdeletion of chromosome 21 is associated with rearrangement. Neoplasia. 2006; 8:465–9. [PubMed: 16820092]
7. Scheble VJ, Braun M, Beroukhim R, Mermel CH, Ruiz C, Wilbertz T, et al. ERG rearrangement is specific to prostate cancer and does not occur in any other common tumor. Mod Pathol. 2010; 23:1061–7. [PubMed: 20473283]
8. Park K, Dalton JT, Narayanan R, Barbieri CE, Hancock ML, Bostwick DG, et al. TMPRSS2:ERG gene fusion predicts subsequent detection of prostate cancer in patients with high-grade prostatic intraepithelial neoplasia. J Clin Oncol. 2014; 32:206–11. [PubMed: 24297949]
9. Xu B, Chevarie-Davis M, Chevalier S, Scarlata E, Zeizafoun N, Dragomir A, et al. The prognostic role of ERG immunopositivity in prostatic acinar adenocarcinoma: a study including 454 cases and review of the literature. Hum Pathol. 2014; 45:488–97. [PubMed: 24406017]
10. Gopalan A, Leversha MA, Satagopan JM, Zhou Q, Al-Ahmadie HA, Fine SW, et al. TMPRSS2-ERG gene fusion is not associated with outcome in patients treated by prostatectomy. Cancer Res. 2009; 69:1400–6. [PubMed: 19190343]
11. Minner S, Enodien M, Sirma H, Luebke AM, Krohn A, Mayer PS, et al. ERG status is unrelated to PSA recurrence in radically operated prostate cancer in the absence of antihormonal therapy. Clin Cancer Res. 2011; 17:5878–88. [PubMed: 21791629]
12. Pettersson A, Graff RE, Bauer SR, Pitt MJ, Lis RT, Stack EC, et al. The TMPRSS2:ERG rearrangement, ERG expression, and prostate cancer outcomes: a cohort study and meta-analysis. Cancer Epidemiol Biomarkers Prev. 2012; 21:1497–509. [PubMed: 22736790]
13. Attard G, Clark J, Ambroisine L, Fisher G, Kovacs G, Flohr P, et al. Duplication of the fusion of TMPRSS2 to ERG sequences identifies fatal human prostate cancer. Oncogene. 2008; 27:253–63. [PubMed: 17637754]
14. Mehra R, Tomlins SA, Yu J, Cao X, Wang L, Menon A, et al. Characterization of TMPRSS2-ETS gene aberrations in androgen-independent metastatic prostate cancer. Cancer Res. 2008; 68:3584–90. [PubMed: 18483239]

15. Foos G, Hauser CA. Altered Ets transcription factor activity in prostate tumor cells inhibits anchorage-independent growth, survival, and invasiveness. Oncogene. 2000; 19:5507–16. [PubMed: 11114728]
16. Grasso CS, Wu YM, Robinson DR, Cao X, Dhanasekaran SM, Khan AP, et al. The mutational landscape of lethal castration-resistant prostate cancer. Nature. 2012; 487:239–43. [PubMed: 22722839]
17. Rubinstein YR, Furusawa T, Lim JH, Postnikov YV, West KL, Birger Y, et al. Chromosomal protein HMGN1 modulates the expression of N-cadherin. Febs J. 2005; 272:5853–63. [PubMed: 16279949]
18. Jaggi M, Nazemi T, Abrahams NA, Baker JJ, Galich A, Smith LM, et al. N-cadherin switching occurs in high Gleason grade prostate cancer. Prostate. 2006; 66:193–9. [PubMed: 16173043]
19. Mushinski JF, Nguyen P, Stevens LM, Khanna C, Lee S, Chung EJ, et al. Inhibition of tumor cell motility by the interferon-inducible GTPase MxA. J Biol Chem. 2009; 284:15206–14. [PubMed: 19297326]
20. Baena E, Shao Z, Linn DE, Glass K, Hamblen MJ, Fujiwara Y, et al. ETV1 directs androgen metabolism and confers aggressive prostate cancer in targeted mice and patients. Genes Dev. 2013; 27:683–98. [PubMed: 23512661]
21. Ittmann M, Huang J, Radaelli E, Martin P, Signoretti S, Sullivan R, et al. Animal models of human prostate cancer: the consensus report of the New York meeting of the Mouse Models of Human Cancers Consortium Prostate Pathology Committee. Cancer Res. 2013; 73:2718–36. [PubMed: 23610450]
22. Park JH, Walls JE, Galvez JJ, Kim M, Abate-Shen C, Shen MM, et al. Prostatic intraepithelial neoplasia in genetically engineered mice. Am J Pathol. 2002; 161:727–35. [PubMed: 12163397]
23. Lukacs RU, Goldstein AS, Lawson DA, Cheng D, Witte ON. Isolation, cultivation and characterization of adult murine prostate stem cells. Nat Protoc. 2010; 5:702–13. [PubMed: 20360765]
24. van Bragt MP, Hu X, Xie Y, Li Z. RUNX1, a transcription factor mutated in breast cancer, controls the fate of ER-positive mammary luminal cells. Elife. 2014; 3:e03881. [PubMed: 25415051]
25. Subramanian A, Tamayo P, Mootha VK, Mukherjee S, Ebert BL, Gillette MA, et al. Gene set enrichment analysis: a knowledge-based approach for interpreting genome-wide expression profiles. Proc Natl Acad Sci U S A. 2005; 102:15545–50. [PubMed: 16199517]
26. Mulholland DJ, Kobayashi N, Ruscetti M, Zhi A, Tran LM, Huang J, et al. Pten loss and RAS/MAPK activation cooperate to promote EMT and metastasis initiated from prostate cancer stem/progenitor cells. Cancer Res. 2012; 72:1878–89. [PubMed: 22350410]
27. Carver BS, Chapinski C, Wongvipat J, Hieronymus H, Chen Y, Chandarlapaty S, et al. Reciprocal feedback regulation of PI3K and androgen receptor signaling in PTEN-deficient prostate cancer. Cancer Cell. 2011; 19:575–86. [PubMed: 21575859]
28. Mulholland DJ, Tran LM, Li Y, Cai H, Morim A, Wang S, et al. Cell autonomous role of PTEN in regulating castration-resistant prostate cancer growth. Cancer Cell. 2011; 19:792–804. [PubMed: 21620777]
29. Mills IG. Maintaining and reprogramming genomic androgen receptor activity in prostate cancer. Nat Rev Cancer. 2014; 14:187–98. [PubMed: 24561445]
30. Taylor BS, Schultz N, Hieronymus H, Gopalan A, Xiao Y, Carver BS, et al. Integrative genomic profiling of human prostate cancer. Cancer Cell. 2010; 18:11–22. [PubMed: 20579941]
31. Pettersson A, Lis RT, Meisner A, Flavin R, Stack EC, Fiorentino M, et al. Modification of the association between obesity and lethal prostate cancer by TMPRSS2:ERG. J Natl Cancer Inst. 2013; 105:1881–90. [PubMed: 24292212]
32. Rostad K, Mannelqvist M, Halvorsen OJ, Oyan AM, Bo TH, Stordrange L, et al. ERG upregulation and related ETS transcription factors in prostate cancer. Int J Oncol. 2007; 30:19–32. [PubMed: 17143509]
33. Tynan JA, Wen F, Muller WJ, Oshima RG. Ets2-dependent microenvironmental support of mouse mammary tumors. Oncogene. 2005; 24:6870–6. [PubMed: 16007139]

34. Kabbout M, Garcia MM, Fujimoto J, Liu DD, Woods D, Chow CW, et al. ETS2 mediated tumor suppressive function and MET oncogene inhibition in human non-small cell lung cancer. Clin Cancer Res. 2013; 19:3383–95. [PubMed: 23659968]
35. Park K, Tomlins SA, Mudaliar KM, Chiu YL, Esgueva R, Mehra R, et al. Antibody-based detection of ERG rearrangement-positive prostate cancer. Neoplasia. 2010; 12:590–8. [PubMed: 20651988]
36. Falzarano SM, Zhou M, Carver P, Tsuzuki T, Simmerman K, He H, et al. ERG gene rearrangement status in prostate cancer detected by immunohistochemistry. Virchows Arch. 2011; 459:441–7. [PubMed: 21773753]
37. Chaux A, Albadine R, Toubaji A, Hicks J, Meeker A, Platz EA, et al. Immunohistochemistry for ERG expression as a surrogate for TMPRSS2-ERG fusion detection in prostatic adenocarcinomas. Am J Surg Pathol. 2011; 35:1014–20. [PubMed: 21677539]
38. Gopalan A, Leversha MA, Dudas ME, Maschino AC, Chang J, Al-Ahmadie HA, et al. TMPRSS2-ERG rearrangement in dominant anterior prostatic tumours: incidence and correlation with ERG immunohistochemistry. Histopathology. 2013; 63:279–86. [PubMed: 23701505]
39. Gsponer JR, Braun M, Scheble VJ, Zellweger T, Bachmann A, Perner S, et al. ERG rearrangement and protein expression in the progression to castration-resistant prostate cancer. Prostate Cancer Prostatic Dis. 2014; 17:126–31. [PubMed: 24469092]
40. Chen Y, Chi P, Rockowitz S, Iaquinta PJ, Shamu T, Shukla S, et al. ETS factors reprogram the androgen receptor cistrome and prime prostate tumorigenesis in response to PTEN loss. Nat Med. 2013; 19:1023–9. [PubMed: 23817021]
41. Setlur SR, Mertz KD, Hoshida Y, Demichelis F, Lupien M, Perner S, et al. Estrogen-dependent signaling in a molecularly distinct subclass of aggressive prostate cancer. J Natl Cancer Inst. 2008; 100:815–25. [PubMed: 18505969]
42. Yu J, Mani RS, Cao Q, Brenner CJ, Cao X, Wang X, et al. An integrated network of androgen receptor, polycomb, and TMPRSS2-ERG gene fusions in prostate cancer progression. Cancer Cell. 2010; 17:443–54. [PubMed: 20478527]
43. Munera J, Cecena G, Jedlicka P, Wankell M, Oshima RG. Ets2 regulates colonic stem cells and sensitivity to tumorigenesis. Stem Cells. 2011; 29:430–9. [PubMed: 21425406]
44. Wei GH, Badis G, Berger MF, Kivioja T, Palin K, Enge M, et al. Genome-wide analysis of ETS-family DNA-binding in vitro and in vivo. Embo J. 2010; 29:2147–60. [PubMed: 20517297]
45. Kunderfranco P, Mello-Grand M, Cangemi R, Pellini S, Mensah A, Albertini V, et al. ETS transcription factors control transcription of EZH2 and epigenetic silencing of the tumor suppressor gene Nkx3.1 in prostate cancer. PLoS ONE. 2010; 5:e10547. [PubMed: 20479932]
46. Aytes A, Mitrofanova A, Kinkade CW, Lefebvre C, Lei M, Phelan V, et al. ETV4 promotes metastasis in response to activation of PI3-kinase and Ras signaling in a mouse model of advanced prostate cancer. Proc Natl Acad Sci U S A. 2013; 110:E3506–15. [PubMed: 23918374]
47. Solimini NL, Xu Q, Mermel CH, Liang AC, Schlabach MR, Luo J, et al. Recurrent hemizygous deletions in cancers may optimize proliferative potential. Science. 2012; 337:104–9. [PubMed: 22628553]

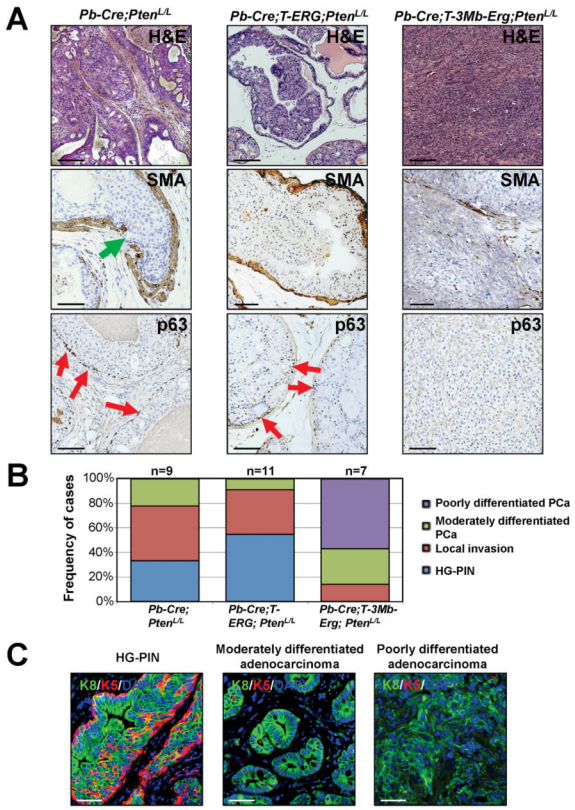

Fig. 1. *Tmprss2-Erg* gene fusion generated through interstitial deletion more strongly cooperates with *Pten*-loss

(A) Representative haematoxylin and eosin (H&E) staining (top row), SMA IHC staining (middle row), and p63 IHC staining (bottom row) of prostate sections from mice with the indicated genotypes. Green arrow denotes discontinuous SMA staining and emergence of epithelial cells through basement membrane. Loss of basal marker p63 was used to validate adenocarcinoma. Red arrows denote p63-expressing ($p63^{+}$) basal cells. Scale bars are 100μm for H&E and 50μm for SMA and p63 staining.

(B) Graphical summary of dominant histological lesions observed in aged mouse models of *Tmprss2-Erg* fusions with (*T-3Mb-Erg*) or without (*T-ERG*) interstitial deletion.

(C) Progressive lesions developed in *Pb-Cre;T-3Mb-Erg;Pten*$^{L/L}$ mice. IF staining for luminal marker K8 (green), basal marker K5 (red), and DAPI (blue) showing progress loss of $K5^{+}$ basal cells in moderately and poorly differentiated adenocarcinomas. Scale bars are 50μm.

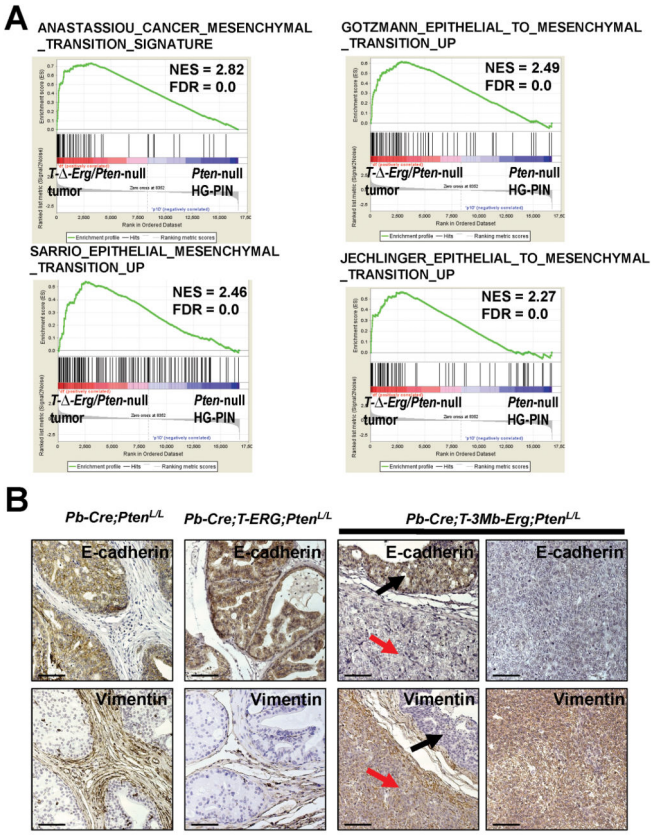

Fig. 2. *T-Δ-Erg/Pten*-null tumors exhibit an EMT phenotype

(A) GSEA results showing highly significant [FDR (i.e., FDR q-val)<0.25] enrichment of multiple EMT gene sets in *T-Δ-Erg/Pten*-null tumors in relation to HG-PIN lesions in *Pb-Cre;Pten*$^{L/L}$ control males. The gene sets are from the c2 CGP (chemical and genetic perturbations) collection of MSigDB (http://www.broadinstitute.org/gsea/msigdb/index.jsp). **(B)** IHC confirmation of EMT features in *T-Δ-Erg/Pten*-null tumors using E-cadherin (top rows) and Vimentin (bottom rows) staining. Control *Pten*-null and *T-ERG/Pten*-null HG-PINs (left panels), *T-Δ-Erg/Pten*-null HG-PIN (middle panel, black arrows), and *T-Δ-Erg/Pten*-null tumors (middle panel, red arrows; right panel) are shown. Scale bars are 50 μm.

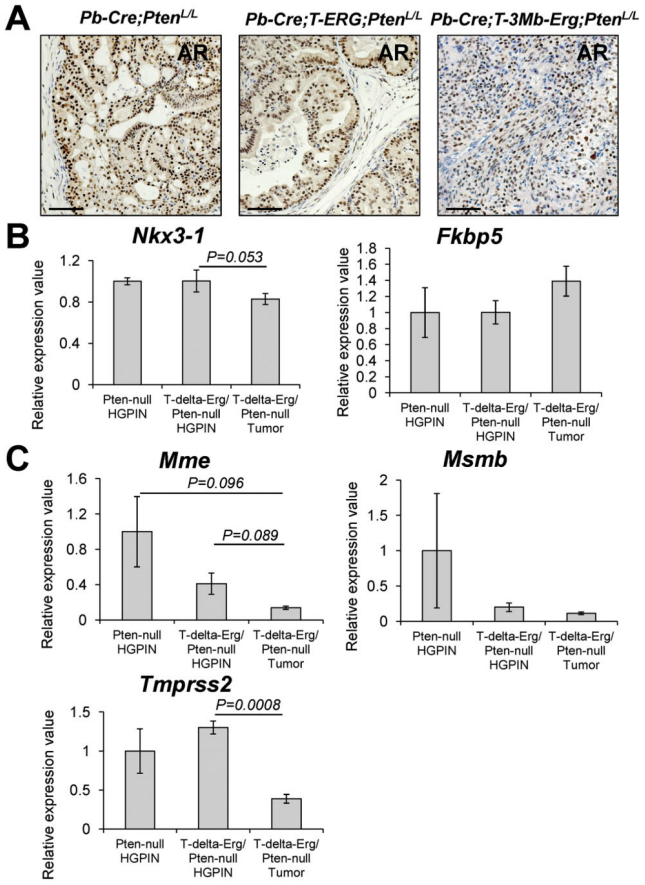

Fig. 3. *T-Δ-Erg/Pten*-null tumors retain AR signaling partially

(A) IHC staining depicting AR expression in typical prostate lesions from various PCa mouse models. Scale bars are 50μm.

(B–C) Relative expression values of AR target genes, *Nkx3-1* and *Fkbp5* (B), as well as *Mme*, *Msmb* and *Tmprss2* (C), in *T-Δ-Erg/Pten*-null tumors and HG-PINs in relation to *Pten*-null HG-PINs (=1), based on microarray expression profiling. Data represent mean ± SEM. *P-values* (Student's t-test) for pairwise comparisons that were significant ($p<0.05$) or marginally significant ($p<0.1$) were shown. All the other comparisons were not statistically significant.

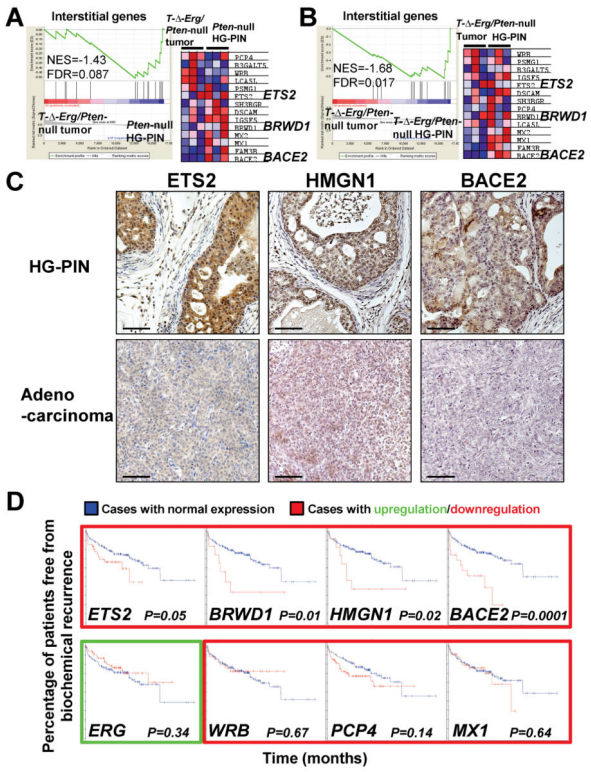

Fig. 4. Multiple interstitial genes are candidate prostate tumor suppressors

(A–B) GSEA for the "Interstitial genes" showing significant (FDR<0.25) negative enrichment (i.e., downregulation) of this gene set in *T-Δ-Erg/Pten*-null tumors in relation to *Pten*-null HG-PINs (A) or *T-Δ-Erg/Pten*-null HG-PINs (B). In A and B, Enrichment plots are shown on the left, heatmaps are shown on the right. In the heatmap, red to pink to light blue to blue indicate highest to lowest expression levels of indicated genes.

(C) Expression of select interstitial genes, *Ets2*, *Hmgn1*, and *Bace2* were significantly lower in adenocarcinoma (bottom row) compared to HG-PIN lesions (top row) in *Pb-Cre;T-3Mb-Erg;Pten*$^{L/L}$ mice. Scale bars are 50μm.

(D) Kaplan-Meier curves of human patient data reveals that downregulation of several interstitial genes (outlined in red) predict biochemical relapse after prostatectomy (top row), whereas some do not (bottom row). *ERG* overexpression (outlined in green) also did not predict recurrence in this cohort. Blue lines depict patients with normal expression while patients with deregulated expression are shown as red lines for each graph.

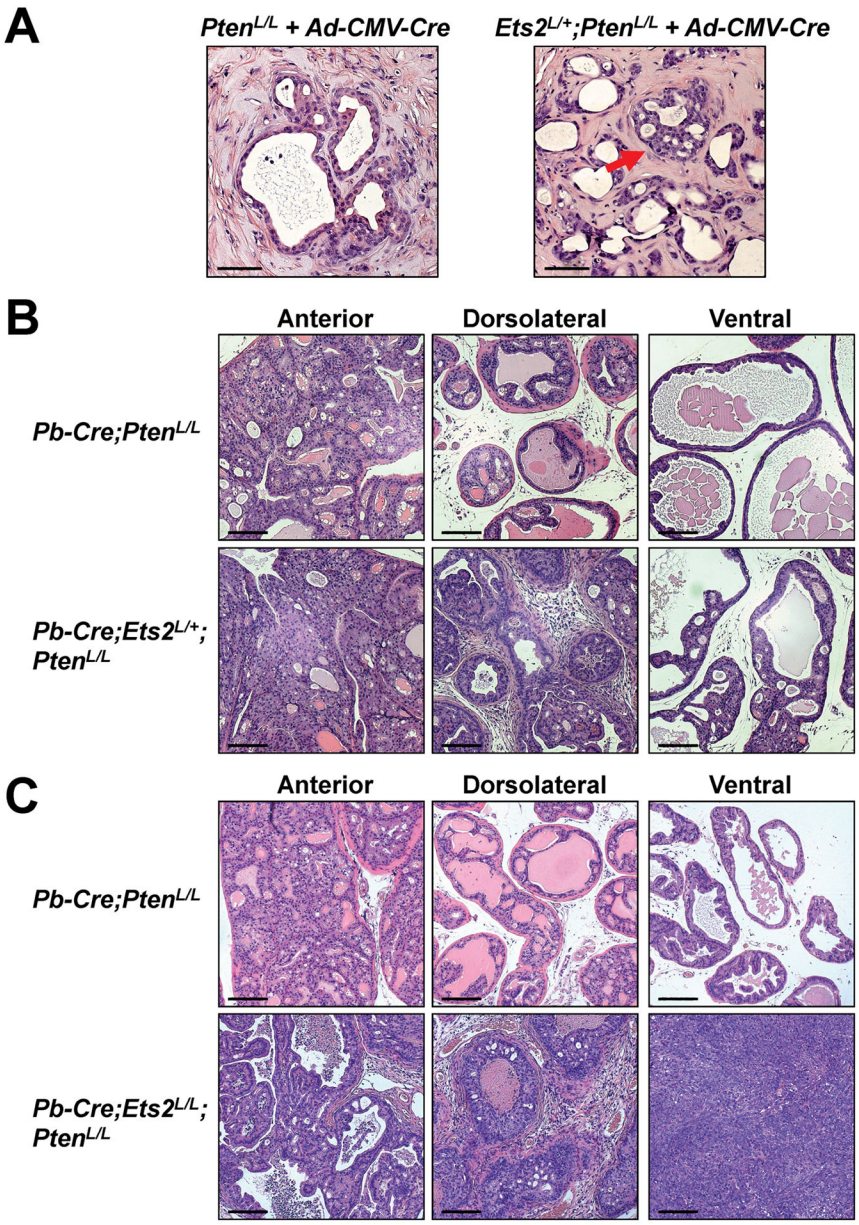

Fig. 5. Reduced dosage of *Ets2* contributes to PCa progression under the *Pten*-null background

(A) Prostate regeneration assay using *Pten*$^{L/L}$ or *Ets2*$^{L/+}$;*Pten*$^{L/L}$ prostate cells infected with *Ad-CMV-Cre* adenovirus prior to implantation. Red arrow denotes a lesion resembling HG-PIN. Scale bars are 50μm.

(B) H&E staining showing enhanced HG-PIN phenotype in a 6-month old *Pb-Cre;Ets2*$^{L/+}$;*Pten*$^{L/L}$ male compared to its age-matched *Pb-Cre;Pten*$^{L/L}$ control male in the dorsolateral and ventral lobes. Scale bars are 100μm.

(C) H&E staining showing invasive PCa and poorly differentiated prostate adenocarcinoma phenotype in a 9-month old *Pb-Cre;Ets2*$^{L/L}$;*Pten*$^{L/L}$ male compared to its age-matched *Pb-Cre;Pten*$^{L/L}$ control male in the dorsolateral and ventral lobes. Scale bars are 100μm.

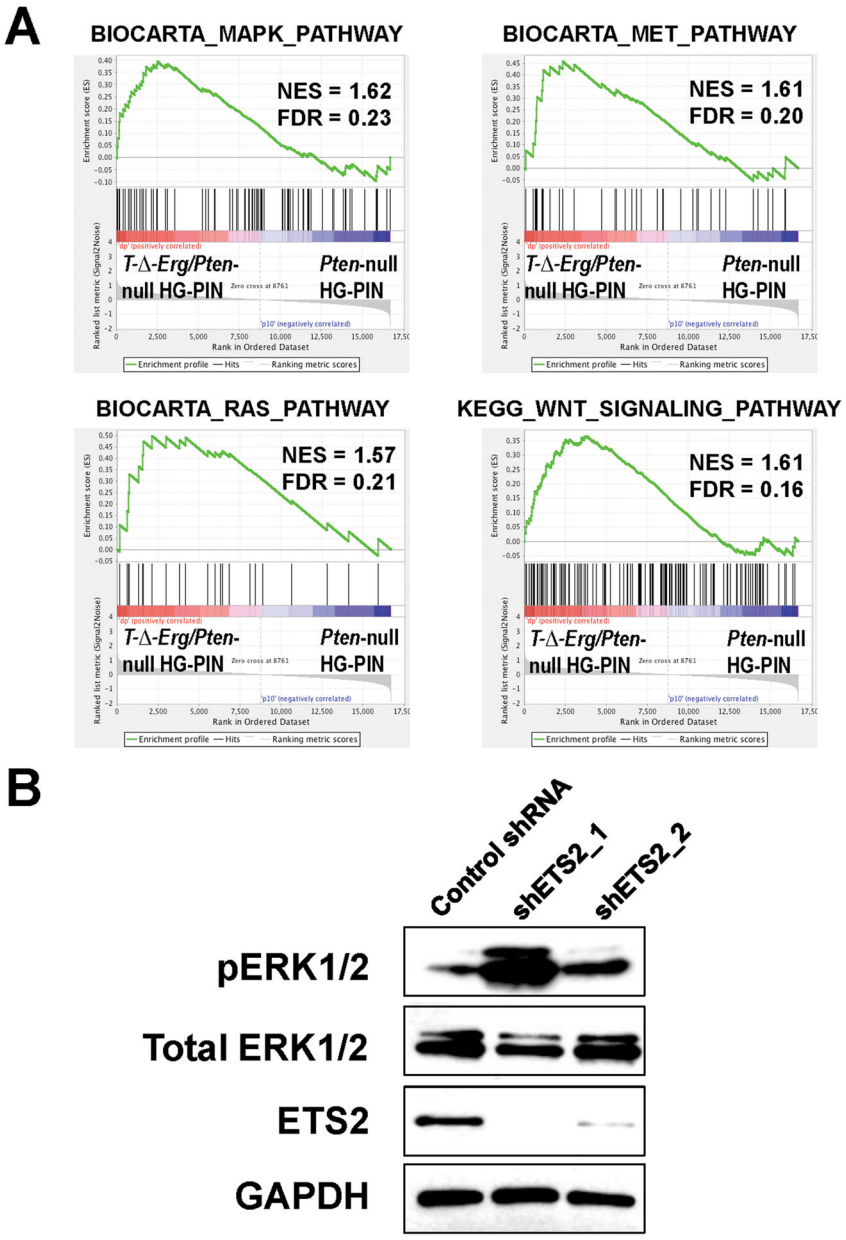

Fig. 6. ETS2-loss leads to activation of the MAPK pathway

(A) GSEA results showing significant (FDR<0.25) enrichment of gene sets related to RAS/MAPK, HGF/MET and WNT signaling in *T-Δ-Erg/Pten*-null HG-PIN lesions in relation to HG-PIN lesions in *Pb-Cre;Pten*$^{L/L}$ control males. Also see Supplementary Table S2 for a complete list of significantly enriched pathway-related gene sets.

(B) Western blot showing increased levels of pERK1/2 in VCaP cells upon knockdown of *ETS2* by two independent shRNAs. Levels of total ERK1/2 and GAPDH were shown as loading controls.

Table 1

Association of select interstitial genes with lethal prostate cancer, Physicians' Health Study and Health Professionals Follow-up Study.

Gene name	*P* value	Expression lower in lethal or indolent?
ERG	0.482	--
ETS2	7.51E-05	Lethal
PSMG1	0.01	Indolent
BRWD1	0.07	Indolent
BRWD1-IT2 (NCRNA00257)	0.204	--
HMGN1	0.059	Indolent
WRB	0.656	--
LCA5L	0.152	--
SH3BGR	0.052	Lethal
C21orf88	0.924	--
B3GALT5	0.041	Lethal
IGSF5	0.173	--
PCP4	0.378	--
DSCAM	0.128	--
BACE2	0.01	Lethal
PLAC4	0.00056	Lethal
FAM3B	0.0017	Lethal
MX2	0.875	--
MX1	0.132	--
TMPRSS2	0.538	--

--no association